Integrated Design of Processes and Products: Optimal Renewable Fuels

Andrea König[a], Lisa Neidhardt[a], Jörn Viell[a], Alexander Mitsos[a,b,c], Manuel Dahmen[b,*]

[a] *Process Systems Engineering (AVT.SVT), RWTH Aachen University, 52074 Aachen, Germany*
[b] *Forschungszentrum Jülich GmbH, Institute for Energy and Climate Research IEK-10: Energy Systems Engineering, 52425 Jülich, Germany*
[c] *JARA-ENERGY, 52056 Aachen, Germany*

Abstract

Integrated product and process design aims at developing innovative products that provide a desired functionality and are produced efficiently. Tailor-made fuels from renewable feedstocks pose a prominent, societally-relevant example. We build upon the integrated design method from Dahmen & Marquardt (2017) and combine it with the production pathway screening tool from Ulonska et al. (2016). We thus design a tailor-made fuel and its optimal production process by minimizing economic and environmental criteria, i.e., cost and global warming impact (GWI). We consider the production of a tailor-made spark-ignition engine fuel from lignocellulosic biomass. Simultaneous process and product design yields optimal multi-component fuels that consist of ethanol, isobutanol, butanone, cyclopentane, and 2-methylfuran with production costs of 18-22 \$ per GJ_{fuel} and GWI values of 38-61 $kg_{CO2eq.}$ per GJ_{fuel}. The proposed method and its solution strategies are, in principle, universal and thus also applicable to products other than fuels.

Keywords: tailor-made fuels; integrated product and process design; fuel design; computer-aided mixture design; Process Network Flux Analysis

[☆] This article is dedicated to Prof. Roger W. H. Sargent, who among his many contributions had advocated for integrated design and optimization of processes more than 50 years ago (Sargent, 1967). We herein present optimization-based design of processes and products.

[*] Corresponding Author: Manuel Dahmen
Email address: m.dahmen@fz-juelich.de (Manuel Dahmen)

1. Introduction

Integrated design of chemical products and processes is concerned with the search for chemical products with desired properties and the development of associated production processes. It aims at a product that is tailored to the intended use and can be produced with high efficiency. A societally-relevant product is given by renewable fuels for advanced, clean, and efficient internal combustion engines (ICEs) as they offer the potential to mitigate climate change and fossil resource dependency.

Chemical product design constitutes one of the two subdisciplines of integrated process and product design with the other one being chemical process design. Chemical product design considers products that are defined by their functionality rather than their molecular structure (Cussler & Moggridge, 2001). It can refer either to the design of novel molecular structures or to the selection and combination of existing candidate structures (Ng & Gani, 2019). If the desired properties cannot be met by a single species, multi-component products are required (Gani, 2004). To design such formulated products, i.e., products formed by a mix of selected components, Conte et al. (2011) have developed a first, generic framework that includes computer-aided design techniques as an essential step.

With road transport currently accounting for half of the OECD's oil demand (Statista, 2017), the design of renewable fuels for advanced, clean and efficient ICEs poses an especially relevant product design problem. Since a single species often cannot fulfil all fuel specifications, fuel design is typically posed as a mixture design problem (Ng & Gani, 2019). In particular, Yunus et al. (2014) have presented a method for formulating gasoline/biofuel blends with maximal biofuel content whereas Ariffin Kashinath et al. (2012) have conducted a blend design study for diesel/biofuel blends that has later been modified and coupled with experimental property validation in a study by Hashim et al. (2017). All three studies focus on product design only. However, tailoring the fuel mixture

properties to engine requirements does not suffice but instead fuel production also needs to be considered to find overall sustainable solutions.

Many mixture design studies implicitly account for the production process by optimizing for cumulative cost of mixture components (Ariffin Kashinath et al., 2012; Conte et al., 2011; Hashim et al., 2017). However, for novel components and processes, component costs and other process-related performance criteria may not be readily available. Furthermore, if the components can be co-produced from a common feedstock in a single process, synergies may arise resulting in lower costs than purchasing the individual species from separate sources. To compute first cost estimates for these cases, (early-stage) process design is required.

At an early stage of process design, many design decisions are not yet fixed. Thus, different raw materials, conversion pathways, unit operations, and operating conditions, are conceivable. These alternative design options can be systematically evaluated using optimization-based methods, i.e., superstructure or network screening approaches (Biegler et al., 1997). Several detailed superstructures have been proposed in the context of biorenewable processing (Garcia & You, 2015; Kong et al., 2016; Giuliano et al., 2016). In particular, Giuliano et al. (2016) have optimized a detailed superstructure for ethanol, succinic acid and levulinic acid production demonstrating the benefits of co-producing bio-based products from a single feedstock. However, if little process data is available, instead of detailed superstructures, first evaluations are typically based only on material balances (Siirola & Rudd, 1971). To this end, rapid screening methods have been developed, e.g., the shortcut method of Bao et al. (2011) or Reaction Network Flux Analysis (RNFA) (Voll & Marquardt, 2012). Extending such mass-based analysis with energy-based evaluation of separation demands, Ulonska et al. (2016) have developed Process Network Flux Analysis (PNFA), an optimization-based method that allows to derive first estimates on investment and operating cost as well as emission criteria such as global warming impact (GWI). PNFA has recently been adapted to better allow for feedstock comparisons in a large process screening for the production of 13 renewable

single-component fuels (König et al., 2019). However, as PNFA is no product design method, it requires *a priori* specification of a chemical product.

Moving towards more integrated evaluations of product and production process design, Ng et al. (2015) have presented a two-stage method that first optimizes the product mixture and then determines the optimal production scheme. Similarly, Hechinger et al. (2010) have proposed sequential strategies that link fuel design with production pathway screening, i.e., RNFA. However, as neither method performs simultaneous process and product design, they do not fully capture the interplay between an efficient production and feasible product compositions. To explore both process-related and product-related degrees of freedom at the same time, a stronger integration of process and product design has often been envisaged (Grossmann, 2004; Victoria Villeda et al., 2012), but hardly realized.

A simultaneous design approach for biofuel/gasoline blends is proposed by Marvin et al. (2013) who optimize reaction pathways of an automatically constructed reaction network under simultaneous consideration of linear fuel property models. Using more detailed property models that account for nonideal thermodynamics, Dahmen & Marquardt (2017) present a simultaneous product and reaction pathway design method that formulates multi-component biofuels. However, like Marvin et al. (2013), the pathway model assumes ideal and instantaneous separations of by-products and does not account for process energy demands, i.e., heating, cooling, and electricity duties. Due to this simplified pathway evaluation, Dahmen & Marquardt (2017) could not perform fuel design by explicitly taking into account economic process-related performance criteria nor could they estimate process emissions.

In summary, so far no integrated product and production process design method has been proposed which can optimize both processing routes and multi-component products considering highly-relevant objectives such as cost and GWI. To overcome this gap, we adapt the simultaneous design approach by Dahmen & Marquardt (2017) and combine it with the pathway model of PNFA (Ulonska et al., 2016; König et al., 2019) thus enabling cost and GWI

estimation. Our focus is on multi-component fuels that are formulated based on a list of pre-specified candidate components. In principle, however, the method is universal and can thus also be applied to products other than fuels.

The remaining paper is structured as follows. First, we describe our method as well as the solution strategy. Then, we apply the proposed method to a case study on the design of bio-based multi-component fuels for advanced spark-ignition (SI) engines. Finally, concluding remarks are given.

2. Method: Integrated Process and Fuel Design

We combine the integrated design approach by Dahmen & Marquardt (2017) with the process pathway model of PNFA (Ulonska et al., 2016; König et al., 2019). Fig. 1 gives an overview of the individual elements of prior work and their combination in this study. The pathway model by Dahmen & Marquardt (2017) is substituted with that of PNFA allowing for a more detailed pathway evaluation based on process energy demands of reactions and separations. This enables minimizing cost and GWI. In the following, we present the pathway model, the fuel property models, and finally the complete optimization problem as well as the corresponding solution strategies.

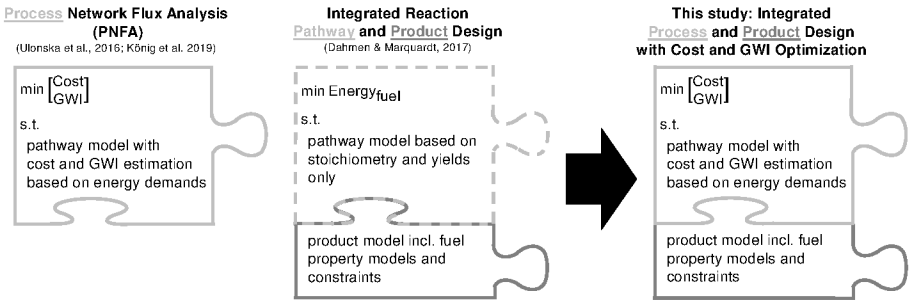

Figure 1: Overview of the individual elements of prior work and their combination in the new method. The product model (dark gray) is adapted from the integrated model by Dahmen & Marquardt (2017) whereas Process Network Flux Analysis (PNFA) (Ulonska et al., 2016; König et al., 2019) (light gray) substitutes the previous pathway model by Dahmen & Marquardt (2017) (dashed, light gray).

2.1. Pathway Model

Our pathway model is based on PNFA (Ulonska et al., 2016; König et al., 2019), a pathway screening method which evaluates not only reaction pathways but also downstream processing options and associated process energy demands thus allowing for cost and GWI estimation.

In the pathway model, products are connected to feedstocks via conversion steps and intermediate products. All considered pathway options and associated components can be represented by a reaction network where nodes symbolize compounds and edges denote conversion steps. For each compound of the network, mole balances are formulated which rely on stoichiometry and yield data thus mapping conversion fluxes and components to each other (Ulonska et al., 2016; König et al., 2019). A detailed description of the mole balance equations is found in the Supplementary Material in section 1.1.1.

Like PNFA, the proposed pathway model incorporates process energy demands of reactions and separations. These energy demands include heating, cooling, and electricity duties which are calculated *a priori* for each conversion step. With respect to reaction pathways, the specific heating and cooling duties are approximated by the respective heat of reaction whereas the specific electricity duty is considered for high-pressure gas-phase reactions assuming a polytropic process (Biegler et al., 1997; Ulonska et al., 2016). With respect to separation steps, energy demands are determined by means of thermodynamically-sound, reduced-order separation models, e.g., Rectification Body Method (RBM) (Bausa et al., 1998; Kraemer et al., 2011), a pinch-based method capable of analyzing zeotropic and (hetero-)azeotropic distillation considering the NRTL model for estimating activity coefficients. For such thermal separations, heat integration is considered in the form of optional vapor recompression (VRC). Other measures of heat integration, e.g., pinch analysis or combustion of waste materials for internal energy supply are not included in this work. For a more detailed description of the energy demand calculations the reader is referred to section 1.1.2 of the Supplementary Material.

Based on the mole balances and process energy demands, production costs

can be estimated. These incorporate raw material costs (biomass and auxiliary feedstock costs), waste disposal costs, investment costs, and utility costs (steam, cooling water, and electricity costs). In contrast to PNFA, we use the continuous, empirical investment cost correlation proposed by Lange (2001),

$$\mathrm{IC} = \frac{\mathrm{CEPCI}_{2016}}{\mathrm{CEPCI}_{1993}} \cdot 2.9 \cdot (E_{\text{transfer duty}}\ [\mathrm{MW}])^{0.55} \qquad [\text{million \$}], \qquad (1)$$

that links the investment costs, IC, to the energy transfer duties of the process ($E_{\text{transfer duty}}$) that are in turn based on the process energy demands (Lange, 2001). Furthermore, the investment costs are updated from 1993-$ to 2016-$ by means of the Chemical Engineering Plant Cost Index, CEPCI. Lange's estimates (cf. Eq. 1) are ranked among the most accurate ones as shown by Tsagkari et al. (2016) who compare six early-stage costing methods to actual costs from existing or planned biorefineries. A more detailed description of the equations used for cost estimation is given in section 1.1.3 of the Supplementary Material.

In addition to a first economic evaluation, we also analyze environmental measures. While simple mass-based criteria like raw material efficiency measures are conceivable (Voll, 2014), climate researchers often refer to emission-related indicators such as GWI (in former PNFA publications (König et al., 2019; Ulonska et al., 2018, 2016) less precisely called global warming potential (GWP)) as an environmental sustainability measure. We calculate GWI by taking into account emissions of the required utilities (Ulonska et al., 2016) and emissions related to upstream burdens of the feedstocks, i.e., chemical processing steps required for producing feedstocks such as hydrogen (König et al., 2019). We neglect emissions related to feedstock transportation as the focus is strictly on evaluating the chemical conversion pathways. Hence, in contrast to detailed Life Cycle Assessment, our pathway model only provides a rough emission estimate, appropriate for early-stage process design. We use a well-to-wheel system boundary that assumes that all carbon stored in the feedstock is released back into the atmosphere during fuel combustion. The associated model equations are summarized in section 1.1.4 of the Supplementary Material.

2.2. Product Model

A product model consisting of fuel property models ensures that the formulated mixture meets the desired specifications, i.e., a set of physico-chemical fuel properties. An overview of the fuel properties considered in this work and their influence on engine performance is given in Tab. 1.

Table 1: Engine requirements and corresponding fuel properties from Dahmen & Marquardt (2017)

Engine requirement	Fuel property
auto-ignition/knock resistance	derived cetane number DCN [-]
soot emissions	oxygen content O2 [wt-%]
in-cylinder mixture formation	surface tension σ $\left[\frac{\mathrm{mN}}{\mathrm{m}}\right]$ kinematic viscosity ν $\left[\frac{\mathrm{mm}^2}{\mathrm{s}}\right]$ enthalpy of vaporization H_{vap} $\left[\frac{\mathrm{kJ}}{\mathrm{kg}_{\mathrm{air},\Phi=1}}\right]$ Reid vapor pressure p_{Reid} [kPa] distillation curve [°C]

To predict the fuel properties, we use mixture property models that rely on pure-component properties. The latter are determined *a priori* either from experimental data compiled, e.g., by Yanowitz et al. (2017); AIChE (2018), or, if not available, via model-based approaches, e.g., Dahmen & Marquardt (2016); Gmehling (2012). Fuel property models for the derived cetane number (DCN), oxygen content (O2), surface tension (σ), kinematic viscosity (ν), the enthalpy of vaporization (H_{vap}) and the Reid vapor pressure (p_{Reid}) are taken from Dahmen & Marquardt (2017) and can be found in section 1.2 of the Supplementary Material.

In contrast to Dahmen & Marquardt (2017) we use a simplified model for the distillation curve, i.e., the True Boiling Point (TBP) curve (Eckert & Vaněk, 2003; Reiter et al., 2015), to improve the tractability of the resulting optimization problem. Here, the normal boiling points (NBPs) of the pure components approximate the distillation temperature of the mixture. More precisely, the mixture components are first ordered by their NBP. Then, the pure-component

NBPs are mapped to the corresponding cumulated mole fraction interval of each component which are bounded by the cumulated mole fractions, $z_{\mathrm{cum,min},i}$ and $z_{\mathrm{cum,max},i}$ as seen for an exemplary curve in Fig. 2.

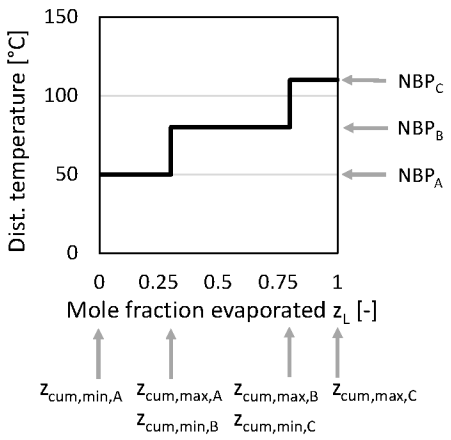

Figure 2: Exemplary True Boiling Point curve for a generic three-component fuel. The three components A, B and C are sorted by their normal boiling points (NBPs), i.e., $\mathrm{NBP_A} = 50°\mathrm{C}$, $\mathrm{NBP_B} = 80°\mathrm{C}$, $\mathrm{NBP_C} = 110°\mathrm{C}$, and mapped according to their mole fractions in the fuel, i.e., 30%, 50%, and 20%, respectively.

The parameter, $0 \leq z_{\mathrm{L}} \leq 1$, which is shown on the x-axis of Fig. 2 represents the distilled mole fraction. Similar to Dahmen & Marquardt (2017), we constrain $\mathrm{TBP}(z_{\mathrm{L}} = 0.1)$=T10m, $\mathrm{TBP}(z_{\mathrm{L}} = 0.5)$=T50m, and $\mathrm{TBP}(z_{\mathrm{L}} = 0.9)$=T90m in the optimization problem with T10m, T50m, and T90m referring to the temperatures where 10, 50, 90 mol-% of the fuel are evaporated, respectively. To comply with standard optimization solvers, we reformulate the nonsmooth function (cf. Fig. 2) by means of integer variables, $y_{i,d}$, that indicate which component i's NBP corresponds to which distillation temperature $d \in \{\mathrm{T10m}, \mathrm{T50m}, \mathrm{T90m}\}$. A detailed description of this implementation is found in section 1.2 of the Supplementary Material.

2.3. Optimization Problem and Solution Strategies

The optimization problem is formulated with specific cost, C_{spec}, in \$ per GJ_{fuel} and specific GWI, GWI_{spec}, in $kg_{CO2\ eq.}$ per GJ_{fuel} as objectives. To determine the specific cost and GWI, overall production cost $C_{overall}$ and overall GWI are divided by a fixed annual fuel production of $\alpha = 2.77 \cdot 10^{12}$ kJ per year. This value equals approx. 100,000 tons of ethanol per year and can be calculated using the lower heating value, i.e., enthalpy of combustion H_{comb}, of the produced fuel components (cf. Eq. S3 in the Supplementary Material). If other production scales were considered, absolute fuel cost would change due to economies of scale, however, this type of analysis is beyond the scope of the current study. The complete optimization problem reads:

$$
\begin{aligned}
\min \quad & \begin{bmatrix} C_{\text{spec}} = \frac{C_{\text{overall}}}{\alpha} & (C_{\text{overall}} \text{ from Eq. S14}) \\ \text{GWI}_{\text{spec}} = \frac{\text{GWI}}{\alpha} & (\text{GWI from Eq. S15}) \end{bmatrix} \\
\text{s.t. pathway model} & \\
& \text{mole balances for products and side products incl. yields (Eqs. S1-S2),} \\
& \text{energy demands of reactions and separations (Eqs. S4-S7),} \\
& \text{raw material costs (Eq. S8)} \\
& \text{waste costs (Eq. S9)} \\
& \text{utility costs (Eq. S10)} \\
& \text{investment costs (Eqs. 1, S12, S13),} \\
& \text{fixed production } \alpha \text{ (Eq. S3)} \\
& \text{fuel property model} \\
& \text{mole and mass fractions of fuel (Eqs. S17 and S19),} \\
& \text{DCN of fuel (Eq. S16),} \\
& \text{oxygen content of fuel (Eq. S18),} \\
& \text{viscosity of fuel (Eqs. S21 and S23),} \\
& \text{surface tension of fuel (Eqs. S20) and S22)} \\
& \text{enthalpy of vaporization of fuel (Eq. S24),} \\
& \text{Reid vapor pressure of fuel (Eqs. S25 and S28),} \\
& \text{distillation curve model: TBP curve (Eqs. S29 - S30, S33 - S36)} \\
& \text{nonnegativity constraints for fluxes and products} \\
& \boldsymbol{y} \in \{0, 1\}.
\end{aligned}
\tag{2}
$$

We implement the resulting mixed-integer nonlinear program in GAMS V25.1.1 (GAMS Development Corporation, 2018) and solve it using the deterministic global solver BARON V18.5.8 (Kılınç & Sahinidis, 2017; Tawarmalani

& Sahinidis, 2005) with standard subsolver settings. We set branching priorities to some of the variables that are present in the nonlinear mixing rules, i.e., a branching priority of 100 for the activity coefficients needed for Reid vapor pressure calculation, a branching priority of 100 to mole fractions, and a branching priority of 30 to the molar product flux vector. The relative solving tolerance is set to 0.01.

We convert the multi-objective optimization problem of Eq. 2 into single objective problems by means of the ϵ-constraint method (Haimes et al., 1971). To improve the initial search for feasible solutions, the problem is initialized by first solving the fuel property model using a dummy objective of zero. Subsequently, for the feasible fuel, we optimize the process variables with respect to cost using the pathway model only. Finally, we use the solution as an initial point to the complete problem of Eq. 2. Similar to Dahmen & Marquardt (2017), we check the miscibility of the resulting multi-component fuel at a temperature of 25°C and atmospheric pressure by minimizing the tangent plane distance function (Baker et al., 1982; Michelsen, 1982) *a posteriori*.

For comparison, we also implement a sequential approach for the point of minimal cost, i.e., the Pareto-optimal solution with lowest cost, and the point of minimal GWI, i.e., the Pareto-optimal solution with lowest GWI. It follows the idea of an iterative cycle for integrated product and process design by Hechinger et al. (2010) and is illustrated in Fig. S1 of the Supplementary Material. In the first step of the sequential strategy, minimal costs (GWIs) of the individual fuel components are determined using only the pathway model. These minimal individual component costs (GWIs) are then passed on to Step 2, where the fuel composition is optimized for a fixed production volume α under consideration of only the product model and by a weighted average of the individual component costs (GWIs). The resulting optimal composition represents a feasible fuel, however, the weighted average of the individual component costs (GWIs) may overstate the costs (GWIs) that could be achieved by co-producing all fuel components in one plant from the same feedstock. Thus, in Step 3, PNFA is used again to optimize the pathways for the fixed fuel composition obtained

from Step 2.

3. Tailor-Made Biofuels for Advanced Spark-Ignition Engines

The proposed method is applied to tailor-made fuels for advanced highly boosted direct-injection SI engines which aim for high efficiency and low pollutant emissions (Hoppe et al., 2015). The fuel specifications seen in Tab. 2 are considered.

Table 2: Fuel property specifications for a highly boosted direct-injection SI engine (adapted from Dahmen & Marquardt (2017)).

Fuel Property	min	max
derived cetane number DCN [-]	–	10
oxygen content O2 [wt-%]	10	–
surface tension σ $\left[\frac{\mathrm{mN}}{\mathrm{m}}\right]$	–	30
kinematic viscosity ν $\left[\frac{\mathrm{mm}^2}{\mathrm{s}}\right]$	0.5	2.0
enthalpy of vaporization H_{vap} $\left[\frac{\mathrm{kJ}}{\mathrm{kg}_{\mathrm{air},\Phi=1}}\right]$	–	60
Reid vapor pressure p_{Reid} [kPa]	45	100
distillation curve		
temperature at 10 mol-% evaporated T10m [°C]	45	70
temperature at 50 mol-% evaporated T50m [°C]	65	125
temperature at 90 mol-% evaporated T90m [°C]	65	190

We consider seven potential fuel components, i.e., ethanol, isobutanol, 2-butanone, 2-methylfuran (2-MF), 2,5-dimethylfuran (2,5-DMF), cyclopentanone, and cyclopentane which can be derived from lignocellulosic biomass. Important properties of the seven potential components are summarized in Tab. S8 of the Supplementary Material.

Fig. 3 shows the reaction network. For simplicity, conversion steps for mixing and separations are not shown. Lignocellulosic biomass is the main raw material with an assumed composition similar to that of beech wood, i.e., 47.7 mol-% cellulose (modeled as $C_6H_{10}O_5$), 35.1 mol-% hemicellulose (modeled as

$C_5H_{10}O_5$), and 17.2 mol-% lignin (modeled as $C_{10}H_{12}O_3$) (Couhert et al., 2009; Dahmen & Marquardt, 2017). All reaction data as well as energy demands for separations are summarized in the Supplementary Material, Tab. S1-S4.

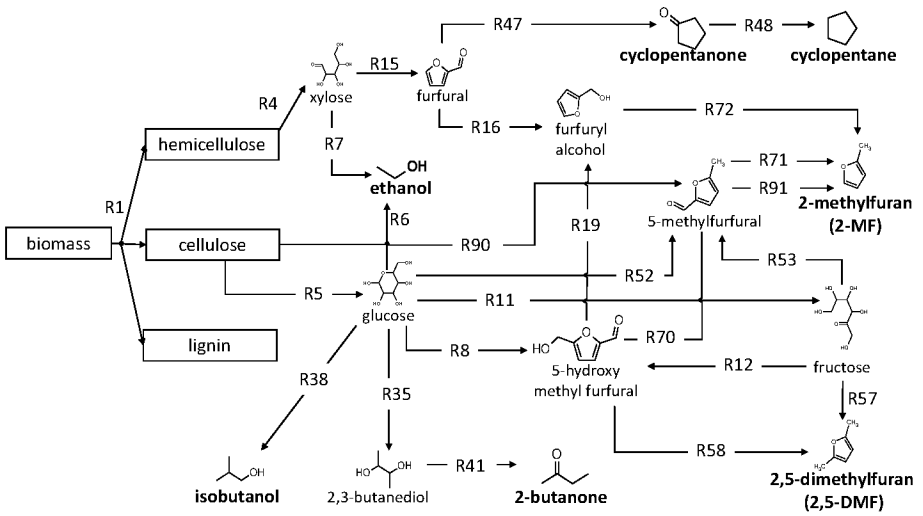

Figure 3: Reaction network: Edges represent reactions; potential fuel species are written in bold. For simplicity, mixing and separation steps as well as CO_2, O_2, and H_2 fluxes are omitted.

For cost estimation, the investment cost parameters given in Tab. S6 of the Supplementary Material are taken. Furthermore, a price of 50 $ per ton of biomass (Ruth, 2011), an electricity price of 7.5 $-ct per kWh (El-Halwagi, 2012), cooling water price of 6.5 $-ct per m^3 (El-Halwagi, 2012), steam price of 9.5 $ per ton (El-Halwagi, 2012), and waste disposal prices of 216.7 $ per ton (Ulrich & Vasudevan, 2007) are considered. Hydrogen needed, e.g., for production of cyclopentane and cyclopentanone, is assumed to be produced externally from biomass gasification and supplied to the process at a price of 2.8 $ per kg (Ruth, 2011). These prices along with various other solvent and auxiliary price data are summarized in Tab. S5 of the Supplementary Material.

The individual GWI factors for utilities and feedstocks are taken from literature. Specifically, for heat and electricity production, the German industry mix of 2020 (IINAS, 2015) is assumed. For biomass, forest residues with a negligi-

ble global warming impact (IINAS, 2015) are considered whereas hydrogen is associated to approx. 1 kg CO_2 eq. per kg H_2 when accounting for the energy demands of gasifying residual biomass (Mehmeti et al., 2018). The specific values are summarized in Tab. S7 of the Supplementary Material.

To compute Reid vapor pressure and assess phase stability, we estimate NRTL parameters based on COSMO-RS data (COSMOlogic GmbH & Co. KG, 2017) (cf. Tab. S9 of the Supplementary Material).

4. Optimal Fuels via Integrated Process and Fuel Design

Fig. 4 shows the optimization results. The pathway performances of the individual fuel components along with the Pareto front of the optimal multi-component fuels are given Fig. 4a). Fig. 4b) shows a magnified version of the Pareto front of the optimal multi-component fuels determined by simultaneous process and product design. Fig. 4c) presents the composition of the optimal multi-component fuels and Fig. 4d) displays the fuel properties in relation to their lower and upper bound restrictions with active constraints marked in black.

The designed, optimal multi-component fuels exhibit production costs between 18 and 22 \$ per GJ_{fuel} with GWI values between 38 and 61 $kg_{CO2eq.}$ per GJ_{fuel} (cf. Fig. 4a) and b)). All optimal multi-component fuels feature high isobutanol contents. Ethanol, 2-butanone, and cyclopentane are included in the cost-optimal multi-component fuel but are (partially) substituted by 2-MF as GWI decreases (cf. Fig. 4c)). With respect to the fuel properties, Fig. 4d) shows that while all multi-component fuels are highly knock-resistant, i.e., DCN values of 5-8, they are also associated to low Reid vapor pressure, high enthalpy of vaporization, and high viscosities. In the following, these results are further analyzed and set into context.

The GWI values of the optimal multi-component fuels lie below the fossil benchmark of 94 $kg_{CO2eq.}$ per GJ_{fuel} (European Parliament and the Council of the European Union, 2018). However, further potential for GWI reduction exists since future steam and electricity generation is expected to rely on much higher

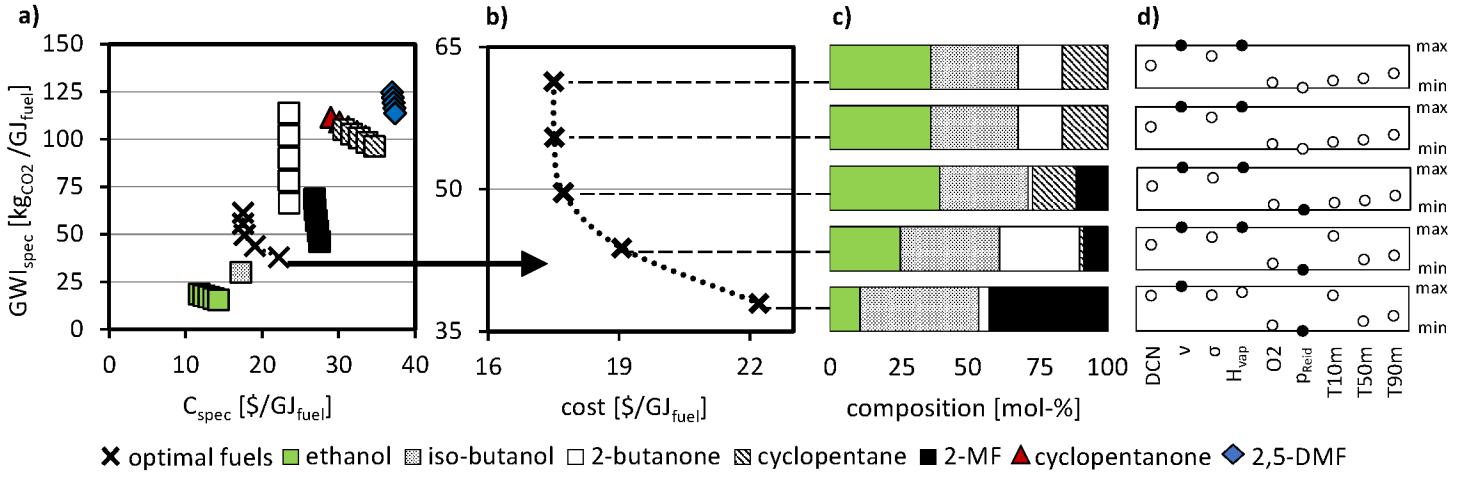

Figure 4: Optimization results: a) Pareto front for individual fuel components (without accounting for fuel specifications) and optimal multi-component fuels, b) Pareto front of only the optimal multi-component fuels determined via simultaneous process and fuel design, c) composition of the optimal fuels, d) fuel properties of optimal fuels; properties that are at their lower or upper bounds are indicated by black dots. Dotted lines are added in the Pareto graph to guide the eye. 2-MF: 2-methylfuran; 2,5-DMF: 2,5-dimethylfuran; DCN: derived cetane number; ν: kinematic viscosity; σ: surface tension; H_{vap}: enthalpy of vaporization; O2: oxygen content, p_{Reid}: Reid vapor pressure; T10m, T50m, T90m distillation curve temperature at 10, 50, 90 mol-% evaporated.

shares of renewables. Considering lower GWI factors would lead to linearly decreased overall GWIs.

The pronounced Pareto front of the multi-component fuels in Fig. 4b) indicates a trade-off between cost and GWI. In the region of minimal cost, the Pareto front is especially steep. This is mainly due to the minor cost benefits of simple un-integrated columns in comparison to heat-integrated VRC columns that exhibit significantly reduced emissions (cf. list of all active conversion fluxes in Tab. S10 of the Supplementary Material).

The results can be further analyzed by setting the optimal fuel composition (cf. Fig. 4c)) into context with the pathway performance of the individual fuel components (cf. Fig. 4a)). The latter have been computed for comparison only, as none of the individual fuel components can meet all the engine requirements specified in Tab. 2. From Fig. 4a) it can be seen that ethanol, followed by isobutanol, exhibits the best pathway performance with low cost and low GWI. Thus, it is plausible that ethanol and isobutanol are present in all optimal multi-component fuels (cf. Fig. 4c)). In case of the cost-optimal multi-component fuel, isobutanol and ethanol are complemented by 2-butanone and cyclopentane. However, 2-butanone and cyclopentane production is associated to rather high emissions due to energy-intensive intermediate separations, i.e., water/2,3-butanediol and water/cyclopentanone separation, respectively. In contrast, 2-MF can reach lower GWI values than 2-butanone and cyclopentane but is associated to higher production costs than 2-butanone (cf. Fig. 4a)). Hence, at the point of minimal GWI, cyclopentane and, in part, 2-butanone are substituted with a larger share of 2-MF (cf. Fig. 4c)) even though this is associated to a reduced share of ethanol to still be able to meet the fuel specifications. Lastly, cyclopentanone and 2,5-DMF are associated to both high cost and high GWI (cf. Fig. 4a)), explaining why they are not added to the optimal fuels.

The properties of the optimal multi-component fuels show the viscosity, the Reid vapor pressure, and the enthalpy of vaporization as limiting factors in this case study since they often/always lie at the respective bounds (cf. black

dots in Fig. 4d)). Considering the pure-component properties (cf. Tab. S8 of the Supplementary Material), it is clear that the high viscosity is mainly caused by isobutanol while ethanol accounts for the high enthalpy of vaporization of the optimal fuels. The Reid vapor pressure is influenced by the low pure-component vapor pressures of the alcohols, especially isobutanol (cf. Tab. S8 of the Supplementary Material), but is, in a mixture, also affected by non-ideal thermodynamics. To meet the fuel property constraints, the alcohols therefore need to be complemented by cyclopentane, 2-butanone, or 2-MF. Cyclopentane, in particular, does not show a favorable pathway performance, i.e., high GWI values and high costs. However, its properties, most importantly its low enthalpy of vaporization and its high volatility, complement the properties of the alcohols.

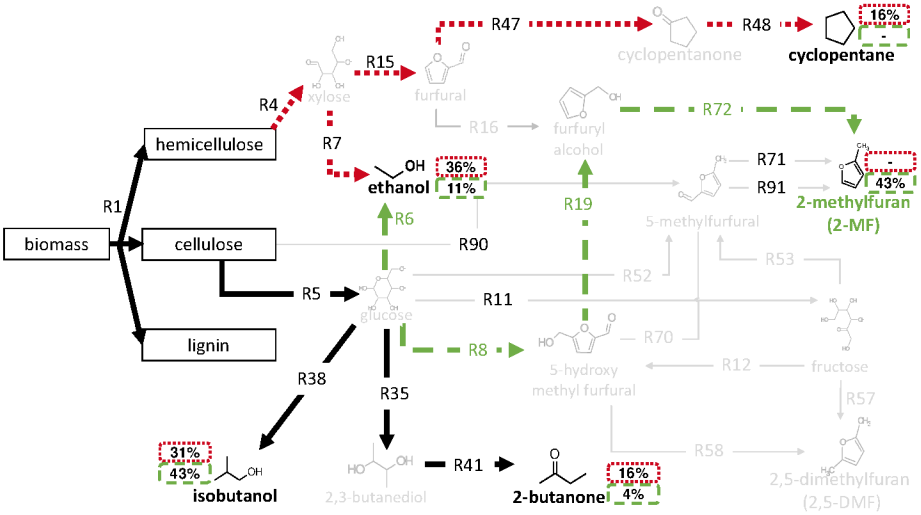

Figure 5: Cost-/GWI-optimal pathway designs and compositions; bold, black, solid routes are activated at both the point of minimal cost and the point of minimal GWI; bold, red, dotted boxes and routes refer only to the design at the point of minimal costs; bold, green, dashed boxes and routes relate only to the design at the point of minimal GWI. Thin, gray routes are not part of the optimal designs. All compositions are given in mol-%.

After analyzing fuel composition and properties, the optimal pathway designs are discussed for two examples, i.e., the point of minimal cost and the point of minimal GWI. The corresponding designs are shown in Fig. 5. At the point of

minimal cost, the fuel consists of 36 mol-% (27 wt-%) ethanol, 31 mol-% (37 wt-%) isobutanol, 16 mol-% (18 wt-%) 2-butanone, and 16 mol-% (18 wt-%) cyclopentane. The cellulose fraction of the biomass feedstock is hydrolyzed to C6-sugars represented by glucose (R5). These are utilized for isobutanol (R38) and 2-butanone production (R35, R41). The hemicellulose fraction is hydrolyzed to C5-sugars represented by xylose (R4) and further converted to cyclopentane (R15, R47, R48) and ethanol (R7). Interestingly, ethanol is not produced from cellulose. This can be explained by the fact that isobutanol and 2-butanone can only be produced from cellulose. Thus, to enable a more efficient use of all biomass fractions and to avoid additional raw material cost, ethanol is produced from the remaining hemicellulose fraction only. At the point of minimal GWI, the fuel consists of 11 mol-% (7 wt-%) ethanol, 43 mol-% (42 wt-%) isobutanol, 4 mol-% (4 wt-%) 2-butanone, and 43 mol-% (47-wt%) 2-MF (cf. Fig. 5). Here, all fuel components, even ethanol, are produced from cellulose. This leads to higher raw material costs but lower energy demands and thus lower emissions.

So far, only the results of the simultaneous design strategy have been presented. Fig. 6 compares them to the results of the sequential approach. It is seen that identical designs are found for the point of minimal GWI, however, results for the point of minimal cost differ. Here, the sequential approach reaches a solution that is suboptimal with costs of 19.1 $ per GJ and GWI of 60 kg CO_2 eq. per GJ compared to cost of 17.5 $ per GJ and a GWI of 61 CO_2 eq. per GJ for the simultaneous approach. This is because the sequential approach does not fully account for the fact that all fuel components share the same common feedstock. Since the optimal fuel composition has been determined based on the costs of the individual components, the fuel designed by the sequential approach consists of more cellulose-based components, i.e., 36% instead of 31% isobutanol, 29% instead of 16% 2-butanone, and 10% instead of 0% 2-MF (cf. Fig. S2 of the Supplementary Material). In particular, hemicellulose-based cyclopentane, which is associated to rather high cost as a single component, can contribute to a more balanced use of all biomass fractions in the simultaneous design while it is not part of the blend in the decomposed approach. This inefficient biomass

use leads to higher overall raw material cost in the sequential approach. For the point of minimal GWI, however, no co-production benefits arise from a more efficient use of biomass as the biomass feedstock is not associated to any upstream emissions and no process utility emissions are assumed for the pretreatment step R1. Hence, both approaches reach the same GWI-optimal designs in this case study. The comparison shows that generally only the simultaneous approach can guarantee optimal solutions as it rigorously addresses the complex interplay of efficient resource utilization and feasible product design. However, the sequential approach is more computationally efficient. Thus, in the future, it could be used for initialization or as a heuristic for large networks that are difficult to solve with the simultaneous approach.

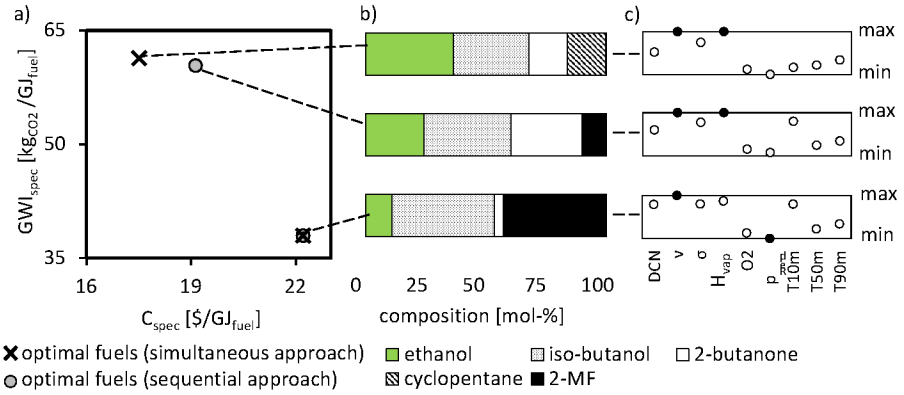

Figure 6: Comparison of simultaneous and sequential approach for the point of minimal cost and the point of minimal GWI: a) optimal multi-component fuels b) composition of optimal fuels, c) fuel properties; properties that are at their lower or upper bounds are indicated by black dots. 2-MF: 2-methylfuran DCN: derived cetane number; ν: kinematic viscosity; σ: surface tension; H_{vap}: enthalpy of vaporization; O2: oxygen content, p_{Reid}: Reid vapor pressure; T10m, T50m, T90m distillation curve temperature at 10, 50, 90 mol-% evaporated.

A posteriori phase stability calculations are conducted for all designed blends. The multi-component fuels that contain 2-MF are predicted to be subject to phase separation whereas those that do not contain 2-MF are predicted to form a single phase. As such phase stability predictions are subject to considerable uncertainty, especially for multi-component mixtures (Gmehling, 2012), these

results should be experimentally validated in the future. If phase separation is confirmed, the blends need to be further refined, e.g., by using stability-enhancing additives such as those investigated by Lapuerta et al. (2007). In principle, rigorous phase separation calculations could also be integrated into the optimization problem. However, this will lead to a bi-level problem and thus substantially increase computational solving effort.

Experimental validation of the designed blends is also desired with respect to the fuel properties, especially those with active lower or upper bounds, i.e., viscosity, heat of vaporization, and Reid vapor pressure. In particular, approximation of the Reid vapor pressure by the bubble point pressure leads to slight overestimates (Dahmen & Marquardt, 2017). In case of meaningful overestimation, raising the bounds of the Reid vapor pressure variable in the optimization problem represents a pragmatic approach that does not increase problem complexity.

Fuel property assessment should prospectively also be augmented with an iterative refinement of the fuel specifications based on detailed understanding of the fuel/engine interactions. To tailor the fuel to the engine and vice versa, it is important that process engineers and engine designers work closely together.

In addition to experimental property refinement and validation, the optimal pathway designs should be further evaluated in conceptual process design. Even though our PNFA-based pathway model is more sophisticated than purely mass-based pathway models, its cost and GWI estimates are expected to be subject to relatively high uncertainties since it is still an early-stage screening method. Primary reasons for this are the rather crude estimation of investment costs, the differing technological maturity of the pathways, and the assumption that lab-scale yield data is representative for the performance of an industrial-scale production process. Some conversion steps also needed to be strongly simplified. In particular, for biomass pretreatment, we assume that the biomass fractions can be separated such that they can be utilized independently of each other. To give an idea of the accuracy of cost and emission estimates obtained from PNFA, Ulonska et al. (2018) have compared the minimum selling prices and

GWIs for ethanol to literature values based on conceptual design. In this study, PNFA estimated cost and GWI in the right order of magnitude (Ulonska et al., 2018). The same conclusion has been drawn for further literature comparisons of isobutanol and ethyl levulinate production cost (Skiborowski, 2018). However, it is still unclear, to which extent these findings can be generalized. To reduce uncertainties, detailed sizing and costing, heat integration, and possibly process intensification measures must be applied.

5. Conclusion

We have presented a new method for integrated design of multi-component fuels and their production processes. The method combines the simultaneous reaction pathway and fuel design approach by Dahmen & Marquardt (2017) with the pathway model from PNFA by Ulonska et al. (2016); König et al. (2019). This enables formulation of tailor-made fuels under consideration of associated production processes on a level of detail that allows for economic as well as environmental optimization. Thus, the proposed model-based approach substitutes early-stage iterative and typically manual design cycles. As a screening tool, it gives first insights on efficient production processes and feasible products.

We designed a variety of Pareto-optimal SI engine biofuels and associated production processes with costs of 18-22 \$ per GJ_{fuel} and GWI values of 38-61 $kg_{CO2eq.}$ per GJ_{fuel}. All optimal fuels consist of more than 50 mol-% ethanol and isobutanol, which are produced at relatively low cost and GWI, complemented by varying amounts of 2-butanone, 2-MF, and cyclopentane to meet the fuel specifications.

The results of the simultaneous pathway and fuel design approach have also been compared to designs of a more computationally-efficient sequential strategy. Even though the sequential approach is not always capable of fully exploiting the synergies arising from co-production of fuel components from a single feedstock, it has yielded near-optimal solutions in our case study. It is therefore considered an interesting option for initialization and use as a heuristic.

Acknowledgement

This work was funded by the Deutsche Forschungsgemeinschaft (DFG, German Research Foundation) under Germany's Excellence Strategy - Exzellenzcluster 2186 "The Fuel Science Center".

Supplementary Materials

The following Supplementary Material is available free of charge and includes:

- Detailed model description
- Pathway model parameters
- NRTL parameters for Reid vapor pressure and phase stability calculations
- Simultaneous vs. sequential approach
- Active fluxes
- Nomenclature of detailed model description

Nomenclature

Abbreviations

2-MF	2-methylfuran
2,5-DMF	2,5-dimethylfuran
CEPCI	Chemical Engineering Plant Cost Index
DCN	derived cetane number
ICE	internal combustion engine
PNFA	Process Network Flux Analysis
RNFA	Reaction Network Flux Analysis
SI	spark ignition
VRC	vapor recompression

Greek Letters

α	design target $[\frac{\text{kJ}}{\text{yr}}]$
ν	kinematic viscosity $[\frac{\text{mm}^2}{\text{s}}]$
σ	surface tension $[\frac{\text{mN}}{\text{m}}]$

Symbols

C	cost $[\frac{\text{million \$}}{\text{yr}}$ or $\frac{\$}{\text{GJ}_{\text{fuel}}}]$
E	energy demand [MW]
GWI	global warming impact $[\text{kg}_{\text{CO}_2,\text{eq}}$ or $\frac{\text{kg}_{\text{CO}_2,\text{eq}}}{\text{GJ}_{\text{fuel}}}]$
H	enthalpy $\left[\frac{\text{kJ}}{\text{kg}_{\text{air},\Phi=1}}\right]$
IC	investment costs [million \$]
NBP	normal boiling point[°C]
O2	oxygen content [wt-%]
p	pressure [kPa]
T10m, T50m,	temperatures in an open batch distillation at 10, 50, 90
T90m	mol-% evaporated [°C]
TBP	true boiling point [°C]
y	integer variable [-]
z	mole fraction [-]

Subscripts

1993, 2016	respective year
cum	cumulated
comb	combustion
d	distillation temperature index
elec	electricity
i	component index
L	liquid
overall	overall

Reid	Reid vapor pressure
spec	specific
transfer duty	transferred energy duty
vap	vaporization

AIChE, 2018. Dippr 801 database version 12.2.0. http://www.aiche.org/dippr (accessed: June 2019).

Ariffin Kashinath, S. A., Abdul Manan, Z., Hashim, H., & Wan Alwi, S. R., 2012. Design of green diesel from biofuels using computer aided technique. Comput. Chem. Eng., 41, 88–92. doi:10.1016/j.compchemeng.2012.03.006.

Baker, L. E., Pierce, A. C., & Luks, K. D., 1982. Gibbs energy analysis of phase equilibria. Soc. Pet. Eng. J., 22, 731–742.

Bao, B., Ng, D. K., Tay, D. H., Jiménez-Gutiérrez, A., & El-Halwagi, M. M., 2011. A shortcut method for the preliminary synthesis of process-technology pathways: An optimization approach and application for the conceptual design of integrated biorefineries. Comput. Chem. Eng., 35, 1374–1383. doi:10.1016/j.compchemeng.2011.04.013.

Bausa, J., Watzdorf, R. v., & Marquardt, W., 1998. Shortcut methods for nonideal multicomponent distillation: I. simple columns. AIChE J., 44, 2181–2198. doi:10.1002/aic.690441008.

Biegler, L. T., Grossmann, I. E., & Westerberg, A. W., 1997. Systematic methods of chemical process design. Prentice-Hall international series in the physical and chemical engineering sciences. Upper Saddle River, NJ: Prentice-Hall.

Conte, E., Gani, R., & Ng, K. M., 2011. Design of formulated products: A systematic methodology. AIChE J., 57, 2431–2449. doi:10.1002/aic.12458.

COSMOlogic GmbH & Co. KG, 2017. COSMOthermX17 VersionC30_1701. www.cosmologic.de (accessed: June 2019).

Couhert, C., Commandre, J.-M., & Salvador, S., 2009. Is it possible to predict gas yields of any biomass after rapid pyrolysis at high temperature from its composition in cellulose, hemicellulose and lignin? Fuel, 88, 408–417. doi:10.1016/j.fuel.2008.09.019.

Cussler, E. L., & Moggridge, G. D., 2001. Chemical product design. Cambridge series in chemical engineering. Cambridge: Cambridge Univ. Press.

Dahmen, M., & Marquardt, W., 2016. Model-based design of tailor-made biofuels. Energy Fuels, 30, 1109–1134. doi:10.1021/acs.energyfuels.5b02674.

Dahmen, M., & Marquardt, W., 2017. Model-based formulation of biofuel blends by simultaneous product and pathway design. Energy Fuels, 31, 4096–4121. doi:10.1021/acs.energyfuels.7b00118.

Eckert, E., & Vaněk, T., 2003. Simulation of separation columns using substitute mixtures. sschi.chtf.stuba.sk/konf2003/abstracts/35.pdf (accessed: June 2019).

El-Halwagi, M. M., 2012. Sustainable design through process integration: Fundamentals and applications to industrial pollution prevention, resource conservation, and profitability enhancement. Boston, MA: Butterworth-Heinemann.

European Parliament and the Council of the European Union, 2018. Directive (EU) 2018/2001 on the promotion of the use of energy from renewable sources. Official Journal of the European Union, (pp. 82–209) https://eur-lex.europa.eu/legal-content/EN/TXT/?uri=uriserv:OJ.L_.2018.328.01.0082.01.ENG&toc=OJ:L:2018:328:TOC (accessed: May 2019).

GAMS Development Corporation, 2018. Gams - general algebraic modeling system v25.1.1. www.gams.com (accessed: June 2019).

Gani, R., 2004. Chemical product design: challenges and opportunities. Comput. Chem. Eng., 28, 2441–2457. doi:10.1016/j.compchemeng.2004.08.010.

Garcia, D. J., & You, F., 2015. Multiobjective optimization of product and process networks: General modeling framework, efficient global optimization algorithm, and case studies on bioconversion. AIChE J., 61, 530–554. doi:10.1002/aic.14666.

Giuliano, A., Cerulli, R., Poletto, M., Raiconi, G., & Barletta, D., 2016. Process pathways optimization for a lignocellulosic biorefinery producing levulinic acid, succinic acid, and ethanol. Ind. Eng. Chem. Res., 55, 10699–10717. doi:10.1021/acs.iecr.6b01454.

Gmehling, J., 2012. Chemical Thermodynamics for Process Simulation. Weinheim, Germany: Wiley-VCH.

Grossmann, I. E., 2004. Challenges in the new millennium: Product discovery and design, enterprise and supply chain optimization, global life cycle assessment. Comput. Chem. Eng., 29, 29–39. doi:10.1016/j.compchemeng.2004.07.016.

Haimes, Y. Y., Lasdon, L. S., & Wismer, D. A., 1971. On a bicriterion formulation of the problems of integrated system identification and system optimization. IEEE Trans. Syst. Man. Cybern., 1, 296–297. doi:10.1109/TSMC.1971.4308298.

Hashim, H., Narayanasamy, M., Yunus, N. A., Shiun, L. J., Muis, Z. A., & Ho, W. S., 2017. A cleaner and greener fuel: Biofuel blend formulation and emission assessment. J. Clean Prod., 146, 208–217. doi:10.1016/j.jclepro.2016.06.021.

Hechinger, M., Voll, A., & Marquardt, W., 2010. Towards an integrated design of biofuels and their production pathways. Comput. Chem. Eng., 34, 1909–1918. doi:10.1016/j.compchemeng.2010.07.035.

Hoppe, F., Heuser, B., Thewes, M., Kremer, F., Pischinger, S., Dahmen, M., Hechinger, M., & Marquardt, W., 2015. Tailor-made fuels for future engine concepts. Int. J. Engine. Res., 17, 16–27. doi:10.1177/1468087415603005.

IINAS, 2015. International Institute for Sustainability Analysis and Strategy – GEMIS Software. http://www.iinas.org/gemis-de.html (accessed: June 2019).

Kılınç, M. R., & Sahinidis, N. V., 2017. Exploiting integrality in the global optimization of mixed-integer nonlinear programming problems with BARON. Optim. Methods. Softw., 33, 540–562. doi:10.1080/10556788.2017.1350178.

Kong, L., Sen, S. M., Henao, C. A., Dumesic, J. A., & Maravelias, C. T., 2016. A superstructure-based framework for simultaneous process synthesis, heat integration, and utility plant design. Comput. Chem. Eng., 91, 68–84. doi:10.1016/j.compchemeng.2016.02.013.

König, A., Ulonska, K., Mitsos, A., & Viell, J., 2019. Optimal applications and combinations of renewable fuel production from biomass and electricity. Energy Fuels, 33, 1659–1672. doi:10.1021/acs.energyfuels.8b03790.

Kraemer, K., Harwardt, A., Skiborowski, M., Mitra, S., & Marquardt, W., 2011. Shortcut-based design of multicomponent heteroazeotropic distillation. Chem. Eng. Res. Des., 89, 1168–1189. doi:10.1016/j.cherd.2011.02.026.

Lange, J.-P., 2001. Fuels and chemicals manufacturing; guidelines for understanding and minimizing the production costs. Cattech, 5, 82–95. doi:10.1023/A:1011944622328.

Lapuerta, M., Armas, O., & García-Contreras, R., 2007. Stability of diesel–bioethanol blends for use in diesel engines. Fuel, 86, 1351–1357. doi:10.1016/j.fuel.2006.11.042.

Marvin, W. A., Rangarajan, S., & Daoutidis, P., 2013. Automated generation and optimal selection of biofuel-gasoline blends and their synthesis routes. Energy Fuels, 27, 3585–3594. doi:10.1021/ef4003318.

Mehmeti, A., Angelis-Dimakis, A., Arampatzis, G., McPhail, S., & Ulgiati, S., 2018. Life cycle assessment and water footprint of hydrogen production

methods: From conventional to emerging technologies. Environments, 5, 24. doi:10.3390/environments5020024.

Michelsen, M. L., 1982. The isothermal flash problem. part I. stability. Fluid Phase Equilib., 9, 1–19. doi:10.1016/0378-3812(82)85001-2.

Ng, K. M., & Gani, R., 2019. Chemical product design: Advances in and proposed directions for research and teaching. Comput. Chem. Eng., 126, 147–156. doi:10.1016/j.compchemeng.2019.04.008.

Ng, L. Y., Andiappan, V., Chemmangattuvalappil, N. G., & Ng, D. K., 2015. A systematic methodology for optimal mixture design in an integrated biorefinery. Comput. Chem. Eng., 81, 288–309. doi:10.1016/j.compchemeng.2015.04.032.

Reiter, A. M., Wallek, T., Pfennig, A., & Zeymer, M., 2015. Surrogate generation and evaluation for diesel fuel. Energy Fuels, 29, 4181–4192. doi:10.1021/acs.energyfuels.5b00422.

Ruth, M., 2011. Hydrogen production cost estimate using biomass gasification: Independent review: Technical report national renewable energy laboratory. https://www.hydrogen.energy.gov/pdfs/51726.pdf (accessed: June 2019).

Sargent, R. W. H., 1967. Integrated design and optimization of processes. Chem. Eng. Prog., 63, 71–78.

Siirola, J. J., & Rudd, D. F., 1971. Computer-aided synthesis of chemical process designs. from reaction path data to the process task network. Ind. Eng. Chem. Fund., 10, 353–362. doi:10.1021/i160039a003.

Skiborowski, K., 2018. Optimization-based Process Screening of Biorefinery Pathways at Early Design Stage. Aachen: Mainz, G.

Statista, 2017. Distribution of oil demand in the OECD in 2017 by sector. https://www.statista.com/statistics/307194/top-oil-consuming-sectors-worldwide/ (accessed: June 2019).

Tawarmalani, M., & Sahinidis, N. V., 2005. A polyhedral branch-and-cut approach to global optimization. Math. Program., 103, 225–249. doi:10.1007/s10107-005-0581-8.

Tsagkari, M., Couturier, J.-L., Kokossis, A., & Dubois, J.-L., 2016. Early-stage capital cost estimation of biorefinery processes: A comparative study of heuristic techniques. ChemSusChem, 9, 2284–2297. doi:10.1002/cssc.201600309.

Ulonska, K., König, A., Klatt, M., Mitsos, A., & Viell, J., 2018. Optimization of multiproduct biorefinery processes under consideration of biomass supply chain management and market developments. Ind. Eng. Chem. Res., 57, 6980–6991. doi:10.1021/acs.iecr.8b00245.

Ulonska, K., Skiborowski, M., Mitsos, A., & Viell, J., 2016. Early-stage evaluation of biorefinery processing pathways using process network flux analysis. AIChE J., 62, 3096–3108 http://dx.doi.org/10.1002/aic.15305. doi:10.1002/aic.15305.

Ulrich, G. D., & Vasudevan, P. T., 2007. Predesign for pollution prevention and control. Chem. Eng. Prog., 6, 53–60 http://www.aiche.org/resources/publications/cep/2007/june/predesign-pollution-prevention-and-control.

Victoria Villeda, J. J., Dahmen, M., Hechinger, M., Voll, A., & Marquardt, W., 2012. Towards model-based design of biofuel value chains. Curr. Opin. Chem. Eng., 1, 465–471. doi:10.1016/j.coche.2012.08.001.

Voll, A., 2014. Model-based screening of reaction pathways for processing of biorenewables. Dissertation RWTH Aachen University Aachen.

Voll, A., & Marquardt, W., 2012. Reaction network flux analysis: Optimization-based evaluation of reaction pathways for biorenewables processing. AIChE J., 58, 1788–1801. doi:10.1002/aic.12704.

Yanowitz, J., Ratcliff, M., McCormick, R., Taylor, J., & Murphy, M., 2017. Compendium of experimental cetane numbers. https://www.nrel.gov/docs/fy17osti/67585.pdf (accessed: June 2019).

Yunus, N. A., Gernaey, K. V., Woodley, J. M., & Gani, R., 2014. A systematic methodology for design of tailor-made blended products. Comput. Chem. Eng., 66, 201–213. doi:10.1016/j.compchemeng.2013.12.011.